Proceedings of the 23rd National Heat and Mass Transfer Conference and 1st International ISHMT-ASTFE Heat and Mass Transfer Conference IHMTC2015
17-20 December, 2015, Thiruvananthapuram, India

Paper No. 2015-799

A NOVEL INTEGRATED COOLING AND HEAT RECOVERY SYSTEM USING ORGANIC RANKINE CYCLE FOR DIESEL ENGINES

Angad S Panesar
School of Computing, Engineering and Mathematics
University of Brighton
a.panesar@brighton.ac.uk

ABSTRACT

Diesel engines offer at least two sources for heat recovery, namely, engine coolant and exhaust gases. The continued trend of cooler engine intake temperatures and engine downsizing now means that the charge air cooling has additionally become a noticeable load on the engine cooling module. There exists key challenges in integrating multiple heat sources, and hence, heat recovery has been typically suggested as an add-on solution using either high temperature heat (i.e. exhaust gases) or low temperature heat (i.e. engine coolant). This paper proposes a novel process integration, termed, the dual process system, to recover exhaust heat and also provide cooling for the charge air. This system is a function of innovative approaches in system architecture (non-isothermal cascade condenser, liquid expander), working fluids (water-organic zeotrope, environment friendly refrigerant) and cycle operation (trilateral flash cycle). The system is simulated using an advanced chemical process modelling tool, Aspen HYSYS. As a case study, steady-state heat recovery was considered at the rated condition from a 12.8 litre engine model. Simulation results showed that the use of the dual process system on new engine platforms can potentially offer 7.2% of additional engine crankshaft power. This corresponded to a 55% increase in power generation compared to the two conventional independent heat recovery cycles targeting the high temperature and the low temperature heat sources.

Keywords: Organic Rankine Cycle, Process Integration, Dual Process System, Aspen HYSYS

NOMENCLATURE

A	Heat transfer area (m^2)
CAC	Charge Air Cooler
E152a	Difluoromethyl-Methyl-Ether
GWP	Global Warming Potential
HEX	Heat exchanger
HT	High Temperature
LT	Low Temperature
$\dot{m}$	Mass flow (kg/s)
NICC	Non-Isothermal Cascade Condenser
ORC	Organic Rankine Cycle
PR	Pressure Ratio
$\dot{Q}$	Thermal load (kW)
R245fa	1,1,1,3,3-Pentafluoropropane
U	Overall heat transfer coefficient ($W/m^2{}^\circ C$)
VFR	Volume Flow Ratio
$\dot{W}$	Power (kW)
W50	50% water 50% acetone by mass
η	Efficiency (%)

INTRODUCTION

Diesel engines are the primary power source for electricity generation and heavy transportation in the 100-1000 kW capacity range. Despite the efforts to directly increase the engine brake thermal efficiency, diesel engines reject 45-55% of the total fuel energy in the form of waste heat at their optimum operating point. Due to increasing CO_2 emissions and fuel costs, coupled with the limited availability of fossil fuels, there is a growing interest in techniques that can even partially utilise this wasted

resource and convert it into usable power. The use of fluid bottoming cycles is regarded as a possible way forward to improve the overall engine specific fuel consumption [1].

Amongst the numerous bottoming cycle options, Organic Rankine Cycles (ORC) using refrigerants (in particular R245fa) are shown to be better adapted to a heat source quality of less than 250°C [2]. On the other hand, traditional Rankine Cycle is suggested to be superior over refrigerants for a heat source quality greater than 450°C [3]. Diesel engines offering different quality and quantity levels of heat sources then present the first challenge in integrating multiple heat sources using a single fluid loop cycle.

Additionally, the specific use of R245fa and water as working fluids are not without challenges. R245fa has a high Global Warming Potential (GWP) of 1030 (relative to CO_2 for an integration time horizon of 100 years) [4]. New regulations requiring the use of lower GWP fluids are already in place in the European mobile air-conditioning sector, and such regulations in the future may also apply to ORCs. Although water offers a thermally stable, non-flammable and environmentally friendly solution, the drawbacks of using water include the high freezing temperature and the requirement of large amounts of superheat to avoid excess liquid post-expansion when using conventional machines [5]. Furthermore, for lower molecular weight fluids like water, turbine design considerations in less than 100 kW output capacities results in lower efficiencies compared to heavier molecular weight organic fluids [6].

Along with the chosen working fluid, the performance of a bottoming cycle strongly correlates with that of the expansion and power generation unit [7]. Single stage scroll expanders, screw expanders and radial turbines have demonstrated design point efficiencies of around 70%, but with relatively lower pressure ratios (below 6:1), inlet pressures (below 30 bar) and inlet temperatures (below 230°C) [8]. Since the pressure ratios required in higher temperature ORCs are larger than those achieved by these three expansion machines, piston expanders are being considered as a valid alternative. Demonstrated piston expanders offer relatively higher pressure ratios (up to 14:1), inlet pressures (up to 50 bar) and inlet temperatures (up to 300°C) [6]. However, despite the recent advancements, the design of low-capacity efficient expansion machines (both positive displacement and dynamic machines) remains a key challenge.

The collective consequence of the above discussed shortcomings and challenges result in low thermal efficiencies and high investment costs of conventional bottoming cycles, tending to a low market acceptance.

Method Overview

In view of the above understanding, a holistic approach, termed process integration, for heat to power conversion was undertaken. Here, process integration is defined as a system oriented approach for optimal energy conversion by plant optimisation. The plant optimisation embraces at least four overlapping fields, these include:

- Selection of suitable working fluids
- Optimisation of cycle operating modes
- Arrangement of the plant thermal and subsystem architecture, and
- Effects on interconnected processes and utilities

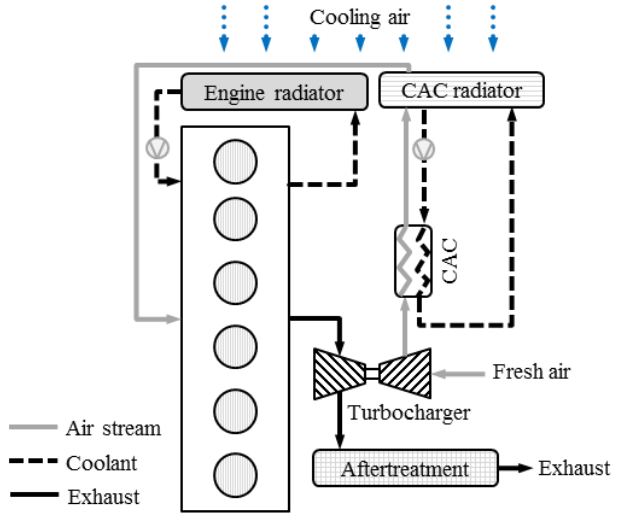

Base engine

$W_{crankshaft}$ = 327 kW
m_{fuel} = 67.3 kg/hr
$\eta_{thermal}$ = 40.6%
$T_{post-aftertreatment}$ = 430°C
$c_{p\ exhaust}$ =1.15 kJ/kg°C
$m_{exhaust}$ = 0.43 kg/s
$P_{exhaust}$ = 1.1 bar

Engine cooling module

$Q_{coolant}$ = 134 kW (115-109°C)
Q_{CAC} = 33 kW (140-65°C)
$Q_{lubricant}$ = 27 kW
$T_{cooling\ air\ inlet}$ = 25°C
$T_{cooling\ air\ exit}$ = 40°C
$\Delta P_{cooling\ fan}$ = 350 Pa
$UA_{engine\ radiator}$ = 2000 W/°C

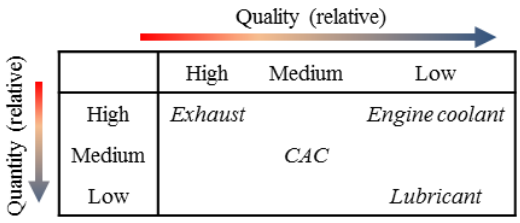

FIGURE 1. ENGINE PLATFORM, PARAMETERS AT THE RATED CONDITION AND HEAT SOURCES

Utilising the above approach, this paper firstly proposes a novel dual process system to partially address the highlighted shortcomings and challenges. This system utilises the findings of previous works and extends the analysis to facilitate the continued examination of

bottoming cycles [9]. Secondly, two independent bottoming cycles targeting all the heat sources on a HDDE, offering a conventional approach, is presented to act as a baseline. Finally, the simulation results of the proposed system are compared to the two independent bottoming cycles. The proposed system is quantitatively evaluated with considerations given to, total heat transfer footprint, size of the expansion machines, system power and system complexity.

Results of a 12.8 liter stationary engine model were used for the bottoming cycle analysis. The schematic of this 6 cylinder, turbocharged engine platform using aftertreatments to meet emission regulations is presented in Fig. 1. The engine performance data at the rated condition and the input variables used in the bottoming cycle analysis are also presented in Fig. 1. Steady-state condition was considered to quantify the improvement in performance. Lubricant heat, which was only 20% of the engine block heat, was excluded from heat recovery considerations owing to combined low quality and quantity levels (Fig. 1).

DUAL PROCESS SYSTEM

System Architecture

It is seen that the charge air cooling has become a noticeable load on the engine cooling module of modern turbocharged diesel engines, and additionally, a potential source for waste heat recovery (Fig. 1). Process integrations that can efficiently exploit both the gaseous waste heat sources, rather than just the exhaust heat, are vital. The system schematic presented in Fig. 2, in association with suggested fluid types and cycle operating modes is proposed as a potential solution. The system utilises two different bottoming cycle concepts and is termed as "dual process system".

The system consists of two distinct temperature-level closed-loop cycles allowing combined heat recovery from two different source quality and quantity levels. The two cycles, the High-Temperature (HT) and the Low-Temperature (LT) cycles are interconnected by a common heat exchanger. The common heat exchanger is a Non-Isothermal Cascade Condenser (NICC). The NICC acts as a condenser for the HT cycle and as a heat source for the LT cycle. The HT cycle recovers the exhaust heat downstream of the aftertreatment devices. The LT cycle recovers the NICC load and the charge air heat in parallel fluid flow. Only the condenser of the LT cycle (cooled by the ambient air) plays a role in dissipating heat out of the system. The bypass lines for the two expanders with pressure reducing valves were excluded for clarity. Furthermore, the storage tanks prior to the two pumps and an exhaust flow bypass valve to control exhaust heat recovery were also omitted.

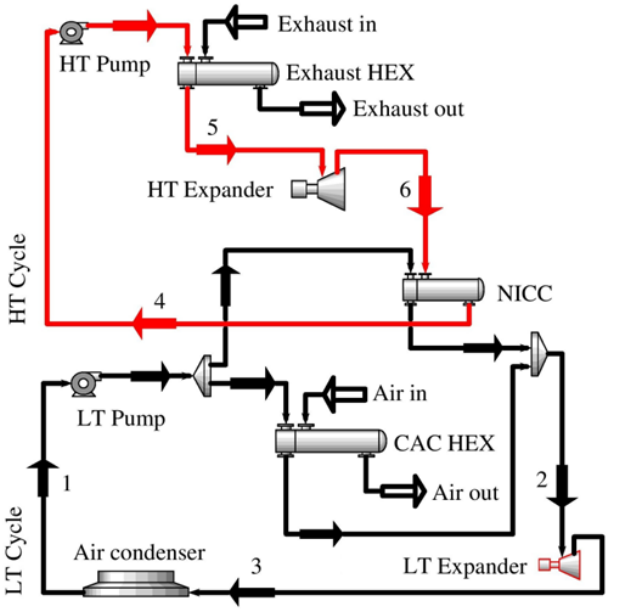

Power elements (fixed)	***Heat transfer elements (fixed)***
$\eta_{HT\ and\ LT\ expander} = 65\%$	$UA_{exhaust\ HEX} = 2500$ W/°C
$\eta_{HT\ and\ LT\ pump} = 55\%$	$UA_{CAC\ HEX} = 2500$ W/°C
$\eta_{transmission} = 90\%$	$UA_{cascade\ cond.} = 6000$ W/°C
$\eta_{cooling\ fan\ and\ motor} = 65\%$	$UA_{air\ cond.} = 7000$ W/°C
$PR_{HT\ expander} = 12{:}1$	$\Delta P_{all\ elements} = 0.3$ bar
$PR_{LT\ expander} = 4{:}1$	

FIGURE 2. ARCHITECTURE OF THE PROPOSED SYSTEM AND DESIGN POINT PARAMETERS

Working Fluids

Due to the high temperature differential across the system, need to limit exergy destruction and design considerations, two distinct working fluids were used in the system. A higher boiling point fluid was used in the HT cycle, while the LT cycle utilised a relatively lower boiling point fluid. Heat source temperatures greater than 450°C thermodynamically support the use of water as a working fluid [5]. However, working fluid selection is more evolved for source temperatures between 350-450°C (i.e. typical exhaust gas temperatures). This is since organic fluids can outperform water, but may still be excluded due to thermal stability considerations [10].

To provide a favourable trade-off, binary water blends may present an alternative avenue. The justification for the use of a miscible, non-reactive, water-organic blend exists since, compared to the pure organic fluid, the blend can offer increased decomposition temperature and heat transfer coefficient, and decreased flammability, fluid cost, negative health and environmental impact. Additionally, blends provide the capability to tailor the system pressures by varying the compositions. As it has been shown that water mixed with similar boiling point organic fluids

demonstrate similar expansion power for a given water mass fraction [9], the selection of a particular blend is more evolved.

A study was conducted to identify water-organic blends with the following primary criterion:

- A water mass fraction of 40-60%: With higher water content, the heat recovery, and hence, the expansion power is shown to reduce when mixed with a higher boiling point (50-100°C) organic fluid [9].
- A homogeneous positive zeotrope with a temperature glide greater than 15°C: Only temperature glides greater than 15°C have demonstrated a noticeable reduction in heat transfer irreversibilities [9].
- A total number of 8-12 atoms in the molecule of the organic blend-constituent: 8-12 atoms in an organic molecule were shown to offer near isentropic vapour curves [9]. When this is mixed with water, the wetness of water is reduced. This ensures that the resulting blend reduces the need of excess superheat to avoid liquid after expansion, and additionally, offer compatibility with the conventional piston expander technology.
- A boiling point of 40-80°C for the organic blend-constituent: A lower blend boiling point will offer super-atmospheric condensation in the HT cycle. The increased condensing pressure will contribute to the use of relatively lower pressure ratio expansion machines.

The screening results, limited to the selection of just one blend that demonstrated the lowest boiling point resulted in the selection of a 50% water and 50% acetone mixture by mass (hereafter referred to as W50). Whereas an earlier identified fluid, Difluoromethyl-Methyl-Ether (E152a), is utilised in the LT cycle [9]. E152a is a hydrofluoroether and belongs to the new generation of refrigerants. It offers a low GWP (110), a low boiling point (-5°C) and a high density (1128 kg/m^3).

Cycle Operation

Figure 2 also summarises the realistic design-point modelling assumptions used for the dual cycle system (for modelling overview refer [11]). The expansion and pumping efficiencies (65, 55%) for both the temperature level cycles were kept constant. Additionally, the HT and the LT expander pressure ratios (12:1, 4:1) were also fixed. The UA (W/°C) values, i.e. overall heat transfer coefficient (U, W/m^2°C) multiplied by the heat transfer area (A, m^2) were kept constant corresponding to a pinch point temperature differences between 10 and 20°C. Under similar process application, this range of pinch point values have demonstrated a suitable trade-off between the required overall heat transfer area and the power produced by the bottoming cycle [9]. The cooling air mass flow for the LT cycle condenser was calculated by limiting the air temperature rise across the condenser to 15°C.

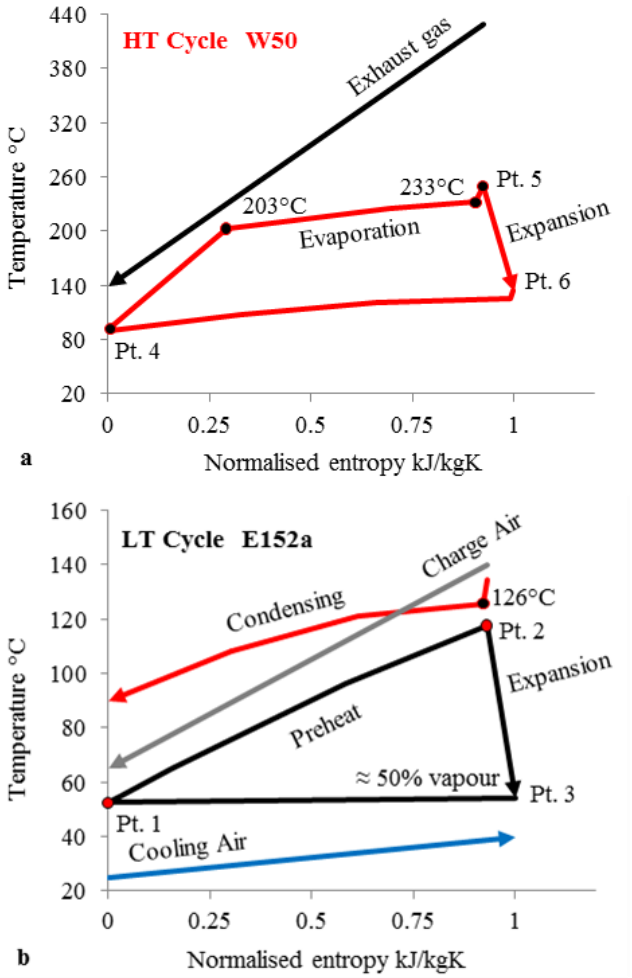

FIGURE 3. T-S DIAGRAM FOR THE HT CYCLE AND THE LT CYCLE IN THE DUAL PROCESS SYSTEM

Figure 3a and b present the Temperature-Entropy (T-S) cycle diagram of the HT and the LT cycle, respectively. In the HT cycle (Fig. 3a), liquid W50 (Pt. 4) was pumped by the HT pump to then be preheated, evaporated and superheated in the exhaust heat exchanger. The superheated vapor (Pt. 5) was then expanded in a vapour expander, the exiting stream (Pt. 6) was then de-superheated, condensed and subcooled in the cascade condenser. The resulting temperature glide of 30°C in W50, which was a function of the blend composition, the absolute pressure and the pressure drop, produced a better temperature match to the exhaust gas, increasing the average heat addition temperature and reducing the exhaust heat exchanger irreversibilities (Fig. 3a). Furthermore during condensation, due to having an increased average heat rejection temperature, W50 offers a larger heat

transfer driving force to achieve the same condensation exit temperature compared to pure and azeotropic fluids. To maintain the relative mass fractions of W50, a slight superheat (17°C) was used. The superheated W50 temperature was limited to 250°C. This was since thermal decomposition in hydrocarbon fluids (and derivatives) was typically reported above this value [12]. Similarly, an additional sub-cooling safety margin was also included prior to HT pump inlet.

In the LT cycle (Fig. 3b), liquid E152a (Pt. 1) was pumped by the LT pump for parallel heat recovery from the charge air heat exchanger and the NICC. The fluid mass flow rate and flow distribution in the two parallel lines were controlled to form a preheated liquid (Pt. 2). This high-pressure, high-temperature, liquid was then expanded in a liquid expander, and exited as a two-phase (Pt. 3). Due to the close similarity to trilateral cycle, the liquid expansion cycle is also termed as trilateral flash cycle. The two-phase, low-pressure, low-temperature E152a was then fully condensed (at a condensing temperature of 52°C) and subcooled in the air cooled condenser. The E152a liquid expansion cycle provided an almost constant temperature difference in the charge air heat exchanger. Furthermore, due to a correct formulation of the blend (i.e. W50), the high temperature glide (36°C) experienced in the NICC offered the added advantage of reduced average condensing temperature of the HT cycle. As the power output of a theoretical bottoming cycle is shown to be up to 4 times more sensitive to an equivalent reduction in heat rejection temperature than to an increase in the heat addition temperature [9]. The heat transfer irreversibilities in both the parallel heat exchangers are limited to relatively lower levels, along with the added crucial thermodynamic advantage offered by the NICC.

Note that, conceptually, the proposed system can be considered as an adaptation of a conventional cascade system [13]. Nonetheless, the behavior of the dual process system is noticeably different. This difference is collectively attributed to the architecture (i.e. NICC and liquid expander), the fluids (i.e. W50 and E152a) and the cycle operation (i.e. trilateral flash cycle).

INDEPENDENT HEAT RECOVERY CYCLES

To compare the system performance and resulting cycle parameters of the proposed dual process system, it was compared against the combined performance of two independent cycles. The first independent cycle, the HT cycle, utilised water to recover the exhaust heat (Fig. 4a). Whereas, the second independent cycle, the LT cycle utilised R245fa to recover engine coolant (50% ethylene glycol, 50% water) and charge air heat in series (Fig. 4b). In order to increase the exergy content of the engine coolant, the coolant temperature was raised to 115°C. Such increases in the coolant temperature have demonstrated no negative effect on the engine efficiency [14].

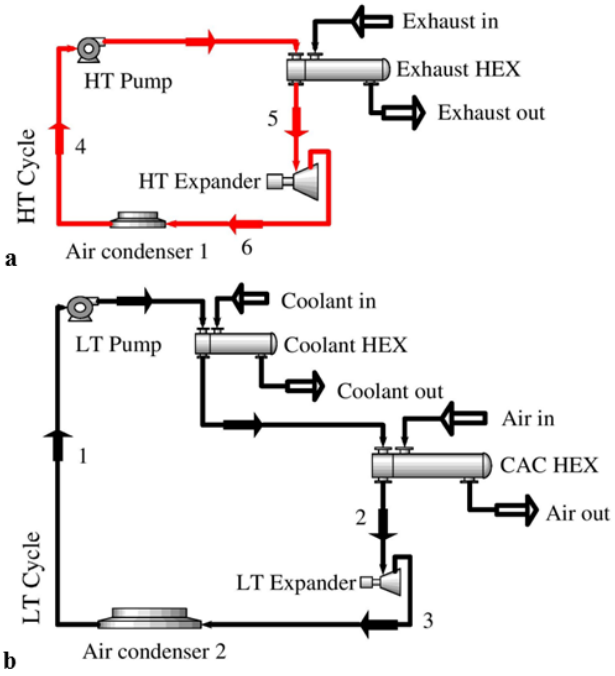

Power elements (fixed)	*Heat transfer elements (fixed)*
$PR_{HT\ expander} = 12{:}1$	$UA_{exhaust\ HEX} = 2500$ W/°C
$PR_{LT\ expander} = 4{:}1$	$UA_{CAC\ HEX} = 2500$ W/°C
	$UA_{Coolant\ HEX} = 6000$ W/°C
	$UA_{air\ cond.\ 1+2} = UA_{air\ cond.}(Fig.\ 2) + UA_{engine\ radiator}(Fig.\ 1)$

FIGURE 4. ARCHITECTURE OF THE INDEPENDENT CYCLES AND SIZING PARAMETERS

To simulate the two independent cycles collectively with a relatively similar system footprint to the dual process cycle, the following was considered. It was assumed that the overall heat transfer coefficient (U) was similar between relatively similar fluid types under similar process application, in particular:

- Exhaust gas/water = Exhaust gas/W50
- Charge air/R245fa = Charge air/E152a
- Coolant/R245fa = W50/E152a
- Cooling air/R245fa = Cooling air/E152a

Therefore, UA (W/C), i.e. overall heat transfer coefficient multiplied by the heat transfer area (A), was considered as a first indicator for similar heat transfer areas. Although this assumption is subjected to inaccuracy [15], nonetheless, as it will be demonstrated, the system power results will be noticeably different for the dual process system and combined performance of the two independent cycles to support this assumption. Additionally, for similar

fluid types (i.e. water, W50 and R245fa, E152a), the expansion pressure ratio was considered as a first indicator of the expansion machine size.

The component isentropic efficiencies and heat exchanger pressure losses were kept same among the proposed system and the independent cycles. Although these efficiencies are a function of the working fluid properties and pressure differential, nonetheless as a first approximation, the considered values may provide an insight into the achievable performance. The cooling air flow temperature rise across both the HT and the LT air condensers was limited to 15°C.

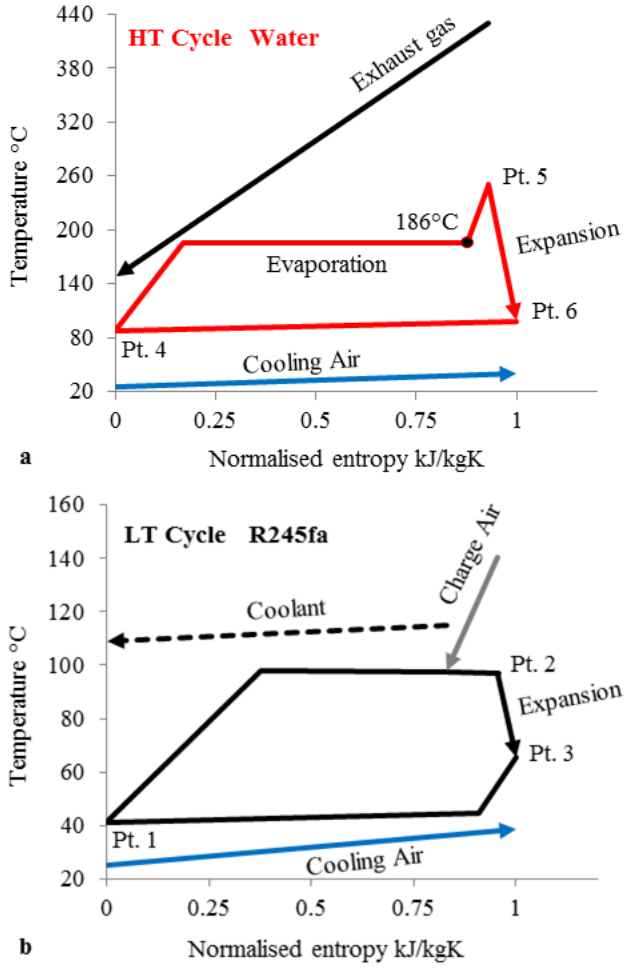

FIGURE 5. T-S DIAGRAM FOR THE INDEPENDENT HT CYCLE AND THE INDEPENDENT LT CYCLE

Figure 4 also summarises the UA values for all the heat transfer elements and pressure ratios for the two expanders corresponding to the same system footprint as that of the dual process system. The only difference being that the combined UA value of the air condensers of the two independent cycles being larger than the dual process air condenser by a value of 2000 W/°C. This was since the two independent cycles also recovered the coolant heat, and the base engine cooling module already included an engine radiator with a value of 2000 W/°C for engine block cooling (Fig. 1). Hence, the absolute condenser sizing of the two independent cycles was higher by this value to perform a like-for-like comparison.

Figure 5a and b presents the T-S cycle diagram of the independent HT water and the independent LT R245fa cycles, respectively. Due to a relatively higher condensing temperature (93°C) in the HT cycle, water was only superheated to 250°C to limit the liquid at expansion exit to below 2%. Furthermore, since R245fa is a drying fluid, a dry saturated vapour expansion was considered in the LT cycle.

RESULTS AND DISCUSSION

Table 1 summarises the system and performance parameters for comparison between the dual process system and the combined two independent cycles from Aspen HYSYS [16]. The volume flow ratio (defined as the ratio between the volumetric flow rates at the expansion outlet to inlet) in the LT cycle expansion from the liquid phase (E152a) were significantly higher than those associated with the expansion of dry saturated vapour (R245fa). Nonetheless, when using twin-screw machines for liquid expansion (or slightly sub-cooled liquid expansion), the overall expansion volume flow ratio using a conventional refrigerant is shown to be over 4.3 times greater than the expander built-in volume flow ratio [17]. As a result, despite the volume flow ratio of LT E152a expander being 21.3:1, the required machine build-in volume flow ratio is expected to be around 5:1. As a result, the engineering challenges, due to the expander size are expected to be low. This value is then similar to the independent LT R245fa cycle recovering combined engine coolant and charge air heat (4.5:1). Furthermore, for equal expansion power, liquid E152a expansion is shown to offer a 30% lower volume flow ratio over liquid R245fa expansion under similar process application, providing a more practical solution [9].

The heat input into the HT (W50) and LT (E152a) cycles in the proposed system were 138.5 and 153.7 kW, giving cycle thermal efficiencies of 12.3 and 9.2%, respectively. Nonetheless, a more appropriate indicator, the combined dual process cycle thermal efficiency, was much higher at 18.2%. This was since around 121.4 kW of the heat input into the LT cycle was internally recuperated. When this is excluded from consideration, and the dual process system is assessed in its entirety, the added heat into the LT cycle from the external source was only 32.3 kW. The internal heat recuperation by the NICC,

combined with the efficient use of the low temperature charge air heat gave an exceptionally high LT cycle thermal efficiency of 43.6% despite a low maximum working fluid temperature (118°C). Although the independent LT (245fa) cycle offered increased heat recovery from the thermal loads on the engine cooling module (137.3 vs. 32.3 kW), the drawback was in its lower cycle thermal efficiency of 7.1%. This independent cycle additionally resulted in the incomplete utilisation of the coolant heat (119.1 vs. 134 kW) and the charge air heat (18.2 vs. 33 kW) due to the mass flow rate limitation. As a result, the dual process cycle thermal efficiency was approximately twice than the combined two independent cycles (18.2 vs. 9.3%). Even more important, the system power, of the dual process system was approximately 55% higher than the combined two independent cycles (23.7 vs. 15.2 kW) despite a 37% lower heat input (170.8 vs. 272.7 kW).

TABLE 1. COMPARISON OF PERFORMANCE AND SYSTEM PARAMETERS

	Dual Process System	Two Independent Cycles
$Q_{Exhaust\ HEX}\ kW$ (HT)	138.5	135.4
$Q_{NICC}\ kW$ (HT)	121.4	-
$Q_{air\ cond.\ 1}\ kW$ (HT)	-	119.8
$P_{max}\ bar$ (HT)	37.1	11.8
$T_{max}\ °C$ (HT)	250	250
$m_{working\ fluid}\ kg/s$ (HT)	0.083	0.053
$VFR_{expander}$ (HT)	9.3:1	8.7:1
$W_{expander}$ (HT)	17.7	15.7
W_{pump} (HT)	0.7	0.1
$\eta_{cycle\ thermal}$ % (HT)	12.3	11.5
$m_{cooling\ air}\ kg/s$ (HT)	-	7.9
W_{fan} (HT)	-	3.7
$Q_{CAC\ HEX}\ kW$ (LT)	32.3	18.2
$Q_{Coolant\ HEX}\ kW$ (LT)	-	119.1
$Q_{air\ cond.}\ kW$ (LT)	139.5	-
$Q_{air\ cond.\ 2}\ kW$ (LT)	-	127.6
$P_{max}\ bar$ (LT)	24.9	12.3
$T_{max}\ °C$ (LT)	118	97
$m_{working\ fluid}\ kg/s$ (LT)	0.251	0.625
$VFR_{expander}$ (LT)	21.3:1	4.5:1
$W_{expander}$ (LT)	18	10.6
W_{pump} (LT)	3.9	0.9
$\eta_{cycle\ thermal}$ % (LT)	9.2	7.1
$m_{cooling\ air}\ kg/s$ (LT)	9.2	8.4
W_{fan} (LT)	4.3	3.9
$\eta_{cycle\ thermal}$ % (Combined)	18.2	9.3
$\eta_{system\ thermal}$ % (Combined)	13.9	5.6
$W_{system}\ kW$ (Combined)	23.7	15.2

Note that the cycle thermal efficiency was calculated according to Eqn. (1). Furthermore, the system power, which attempts to account for the parasitic power and losses, was calculated according to Eqn. (2).

$$\eta_{cycle\ thermal} = (W_{expander} - W_{pump})/Q_{in} \quad (1)$$

$$W_{system} = (W_{HT\ expander} + W_{LT\ expander} - W_{HT\ pump} - W_{LT\ pump})\,\eta_{transmission} - W_{fan} \quad (2)$$

The W50 was simulated using the Wilson property package [18]. The phase change calculations were based on a summation of 15 equal enthalpy intervals to minimise the error in the UA value. Since the W50 characteristics are different from that of a pure fluid, the calculation and design efforts for the exhaust heat exchanger and the NICC are expected to be more complex [5]. Nonetheless, the above results clearly indicate the benefit of the proposed dual process system and support the continued research efforts to implement it in practice. Note that the accurate heat exchanger size comparison (using detailed heat transfer models) and achievable expansion efficiencies (using expander models) remain the limitations of the presented work, and hence, a theme of focus for future works.

CONCLUSION

The present shortcomings and challenges with conventional fluid bottoming cycles for waste heat recovery contribute to the limited deployment of this technology. To partially address this, a holistic approach, termed process integration was undertaken. As a result, a system consisting of two interconnected different temperature-level closed-loop cycles is proposed. The system, termed the dual process system, is a function of innovative approaches in architecture, working fluids and cycle operation. The resulting key advantages and novelty of this system are as follows:

- Improved thermal stability and frost protection: The 50% water by mass in the high temperature cycle mixed with a high critical temperature organic fluid (i.e. acetone, 233°C) bodes well for high temperature heat recovery and offers freezing temperatures similar to the conventional engine coolant. In addition, the low critical temperature pure organic fluid (i.e. E152a, 149°C) in the low temperature cycle experiences a maximum source temperature of 140°C.
- Reduced negative health and environmental impact: This was achieved firstly, using a common laboratory fluid (i.e. acetone) mixed with 50% water, and secondly, using a new generation low global warming refrigerant (i.e. E152a).
- Reduced heat transfer irreversibilities: An important criterion in the water-organic blend selection study

was a high temperature glide. The 30°C glide demonstrated in the high temperature cycle increased the average evaporation temperature and decreased the average condensation temperature. This overcame the limitation of pure and azeotropic fluids during isothermal phase change. In addition, the low temperature cycle utilised liquid expansion, offering an almost parallel temperature match in charge air heat exchanger.

- Higher thermal efficiency: To maintain a high overall thermal efficiency in interconnected cycles, it is vital to maintain high thermal efficiency in the low temperature system section. The use of the non-isothermal cascade condenser efficiently transferred the heat internally in the system, offering a high thermal efficiency in the low temperature cycle, and hence, the overall system (18.2 vs. 9.3%).
- Higher overall conversion efficiency: This was achieved firstly by, dividing the system into two integrated loops based on the temperature range of the available heat sources, and secondly by, using appropriate working fluids combined with suitable cycle operating modes. Additionally, recovering only higher quality exhaust heat reduced the added condenser load, while the increased charge air heat recovery provided lower engine intake temperatures (65 vs. 98°C).

The dual process system showed a significant level of improvement in recoverable power when compared to the two independent heat recovery cycles (23.7 vs. 15.2 kW) for similar overall system footprint and complexity. As a result, the proposed system can provide a higher energy density solution for combined exhaust and charge air heat recovery in future engine platforms with a potential of 7.2% improvement in mechanical power.

ACKNOWLEDGMENTS

The support of faculty members, Morgan Heikal and Robert Morgan is acknowledged.

REFERENCES

[1] Saidur R, Rezaei M, Muzammil WK, Hassan MH, Paria S, and Hasanuzzaman M, 2012. Technologies to recover exhaust heat from internal combustion engines. Renewable and Sustainable Energy Reviews 16:5649-59

[2] Tchanche BF, Lambrinos G, Frangoudakis A, and Papadakis G, 2011. Low-grade heat conversion into power using organic Rankine cycles - A review of various applications. Renewable and Sustainable Energy Reviews 15:3963-79

[3] Sprouse III C, and Depcik C, 2013. Review of organic Rankine cycles for internal combustion engine exhaust waste heat recovery. Appl Therm Eng 51:711-22

[4] Tian H, Shu G, Wei H, Liang X, and Liu L, 2012. Fluids and parameters optimization for the organic Rankine cycles used in exhaust heat recovery of Internal Combustion Engine. Energy 47:125-36

[5] Domingues A, Santos H, and Costa M, 2013. Analysis of vehicle exhaust waste heat recovery potential using a Rankine cycle. Energy 49:71-85

[6] Seher D, Lengenfelder T, Gerhardt J, Eisenmenger N, Hackner M, and Krinn I, 2012. Waste Heat Recovery for Commercial Vehicles with a Rankine Process. In 21st Aachen Colloquium Automobile and Engine Technology, October 8-12, Aachen, Germany

[7] Saadatfar B, Fakhrai R, and Fransson T, 2013. Waste heat recovery Organic Rankine cycles in sustainable energy conversion: A state-of-the-art review. The Journal of MacroTrends in Energy and Sustainability 1

[8] Lopes J, Douglas R, McCullough G, O'Shaughnessy R, and Hanna A, 2012. Review of Rankine Cycle Systems Components for Hybrid Engines Waste Heat Recovery. SAE International, 10.4271/2012-01-1942

[9] Panesar A, 2015. Waste Heat Recovery Using Fluid Bottoming Cycles For Heavy Duty Diesel Engines. PhD Thesis, School of Computing, Engineering and Mathematics, University of Brighton

[10] Yamaguchi T, Aoyagi Y, Osada H, Shimada K, and Uchida N, 2013. BSFC Improvement by Diesel-Rankine Combined Cycle in the High EGR Rate and High Boosted Diesel Engine. SAE Int. J. Engines 6:1275-86

[11] Aspen HYSYS V 7.3, 2011. Unit Operations Guide

[12] Chacartegui R, Sánchez D, Muñoz JM, abd Sánchez T, 2009. Alternative ORC bottoming cycles for combined cycle power plants. Appl Energ 86:2162-70

[13] Wang EH, Zhang HG, Zhao Y, Fan BY, Wu YT, and Mu QH, 2012. Performance analysis of a novel system combining a dual loop organic Rankine cycle (ORC) with a gasoline engine. Energy 43:385-95

[14] Ringler J, Seifert M, Guyotot V, and Hübner W, 2009. Rankine Cycle for Waste Heat Recovery of IC Engines. SAE Int. J. Engines 2:67-76

[15] Perry RH, and Green DW. 2007. Perry's Chemical Engineers' Handbook. McGraw-Hill, ISBN 0070498415

[16] Aspen Technology, 2011. HYSYS V 7.3

[17] Smith IK, 1993. Development of the Trilateral Flash Cycle System: Part 1: Fundamental Considerations. Institution of Mechanical Engineers, Part A: Journal of Power and Energy 207:179-94

[18] Aspen HYSYS V 7.3, 2011. Physical Property Methods